New anti-clogging perspective by discharging sediment from drip irrigation emitters with high-sediment loaded water

Peng Hou [a, b], Jaume Puig-Bargués [c], Lu Liu [a, b], Yang Xiao [a, b], Bo Zhou [a, b], Yunkai Li [a, b *]

a. College of Water Resources and Civil Engineering, China Agricultural University, Beijing 100083, China

b. Engineering Research Center for Agricultural Water-Saving and Water Resources, Ministry of Education, Beijing 100083, China

c. Department of Chemical and Agricultural Engineering and Technology, University of Girona, Girona 17003, Spain

[*] *Yunkai Li* is the corresponding author (E-mail: yunkai@cau.edu.cn)

Abstract: The promotion of drip irrigation technology has been severely constrained by the emitter clogging caused by sediment deposition when using high-sediment loaded water. To fill this gap, a novel solution to the emitter clogging issue has been developed by allowing fine sediment particles to drain as much through the emitter as possible. The sediment deposition and discharge ratio, the sediment discharge rate, and the control threshold for particle size were used to determine the sediment discharge capacity (SDC) of the emitter. The result shows that almost all (>99%) the fine-grained sediment (<100 μm) can be discharged from the flow path of eight emitters, which varied greatly in different emitters. Specifically, pressure compensating emitters (PCE) had higher SDC than non-pressure compensating emitters (NPCE), with relative average flow rate increased by 16.9%-33.0%. Meanwhile, the emitter flow path structure significantly affects SDC. The side wall of the flow path could be changed from a toothed structure to a swirl wash wall optimized structure, which would significantly improve the SDC. Furthermore, the SDC of NPCE was primarily affected by the flow path length (L), and the ratio of the cross-sectional area to the length ($\sqrt{A}/L$). Lastly, stronger emitter SDC closely related to both smaller particle size and concentration of water source. This study presents a fresh idea of sediment treatment for drip irrigation systems with high sediment content water and may contribute to the design of emitters with high sediment discharge capacity, and the effective management and filtration treatment of high-sediment loaded water.

Keywords: drip irrigation; clogging; self-discharge capacity; flow path structure

1. Introduction

The scarcity of irrigation water has become a key obstacle to sustainable agricultural production. High-sediment water (HSW), which can adequately compensate the lack of traditional water resources, is widely distributed throughout the world, in areas such as southwest Europe and northwest China (Puertes et al, 2021; Duker et al, 2020; Niu et al, 2013). Meanwhile, due to the precise and regulated volume of applied irrigation water, drip irrigation is regarded as one of the most effective water-saving methods (Zhou et al, 2019). As a result, the invention of drip irrigation utilizing high-sediment loaded water is regarded as an effective method for solving the problem of water scarcity in agriculture (Qin et al, 2019; Zeng et al, 2018). However, A significant amount of sediment in high-sediment water can easily cause serious clogging of emitters, which impairs distribution uniformity, reduces efficiency and crop productivity, thus, the application and promotion of drip irrigation with high-sediment water is severely constrained by the emitter clogging (EI-Bouhali et al, 2020; Han et al, 2019; Zhang et al, 2017).

Sedimentation and filtration are the most frequently used methods to prevent particles enter into emitter, and thereby they help controlling the emitter clogging in HSW drip irrigation systems (Shen et al, 2022; Bové et al, 2017; Capra et al, 2004). These methods are effective in reducing the coarse-grained sediment, but they are always unsatisfactory for filtering the HSW with primarily fine sediment particles (e.g., the Yellow River water) (Zhang et al, 2021; Puig-Bargués and Lamm, 2013). This is mainly because the slow settling rate of fine sediment particles makes it difficult to treat high concentrations of sediment using the conventional sedimentation and filtration methods (Tao et al., 2017). Moreover, due to the large amount of filter mesh required for fine particle sediment filtering, regular automatic back-washing and high energy consumption are necessary

(Zhang et al., 2021). Therefore, efficient treatment of fine particles of sediment has become the key to alleviate the clogging of HSW drip irrigation emitters.

In fact, fine sediment particles in the water are smaller than the emitter flow path size, usually being less than 1/7 of the flow path size (Liu et al., 2012). This suggested that fine sediment particles could be directly discharged from the emitter flow path. In this case, it could be possible to promote the discharge of fine sediment particles by enhancing the self-discharge capacity of the emitter, and thereby mitigate emitter clogging. Moreover, another advantage of the suggested method was to reduce the requirements of the filtration system. Therefore, the range of sediment particle sizes and concentrations that the emitter can discharge must be further investigated. According to previous studies, emitter clogging was more likely to occur in the case of a sediment particle size of >17 μm, and the risk of emitter clogging increases significantly when the particle size was >30 μm, or when more fine sediment particles are contained (Wu et al., 2014). Besides, it is believed that the sensitive particle size of the labyrinth flow path of the emitter was 0.031-0.038 mm, and that the more sensitive sediment content range was 1.25-1.50 g/L (Niu et al., 2013; Liu et al., 2012). In general, the current research is only targeted at dynamic changes in the silt content and particle size distribution inside the emitter, and there has been no research reported that specifically targets at the evaluation index of the emitter's sediment removal capacity. Also, it is still unclear what influences the emitter self-discharge ability and what the optimization and enhancement method is.

Based on this, an in-situ test on the Yellow River water drip irrigation system emitter clogging was conducted in the river-loop irrigation area, and the difference of sediment particle size and concentration inside the emitter of different structures under different water source particle size and concentration conditions were tested systematically. The objectives of the study were to: (1) present an evaluation index for the sediment self-discharge capacity of the emitter; (2) confirm the factors (e,g., emitter flow path, sediment particle size, sediment concentration) that influence the self-discharge sediment capacity of emitters.

2. Materials and Methods

2.1 Experimental system

This experiment was conducted at Dengkou County Irrigation Experiment Station in the Hetao Irrigation District of Bayannur City, Inner Mongolia Autonomous Region (China). The Yellow River sediment was mixed with water to simulate sandy water sources. The treatments carried out on the irrigation water are shown in Supplementary Material (Table S1). The particle size ranges of the water sources were 0-41 μm, 0-75 μm and 0-100 μm, and the concentration of sediment in water distribution was 1 g/L and 3g/L. Considering the sediment loss during operation, sediment concentration test was conducted once every three days to ensure that the concentration deviation was controlled within 5%. In addition, the water source was replaced once every 6 days.

The drip irrigation pipeline was laid out in the mode of "4 layers + 4 columns". The length of the drip irrigation unit was 15 m, the flow rate inside the drip tape is 0.07-0.11m/s, the emitter is facing upwards. The pressure (0.1 MPa) was maintained at a particular level by gradually regulating and diverting the flow. Filtration system can filter sediment with a particle size of 150um or above, which has no effect on the experimental configuration of the sediment particle size. The flushing flow rate control device was placed at the end of the platform. The system was flushed with a flushing velocity of 0.45m/s during 6 min every 80 h of operation. Combining the ISO standard (ISO 9261) of clogging test methods for emitters and the clogging determination criteria studied by Pei et al (2014), the experimental system test was operated for 10 h per day and the system was operated for a total of 640 h.

Consistent with Muhammad et al. (2021), the test platform is mainly composed of three parts (including the water source, the filtration system, and the drip irrigation unit), as shown in Fig. 1. The system operation mode is shown in Supplementary Material. The experimental system run 10 h per day up to a total operation time of 640 h. Eight flat emitters with different structure were hereby selected. Non-pressure compensating emitters (NPC) with toothed flow path (NPCL) of 1.0 L/h, 1.4 L/h and 1.6 L/h flow rate, respectively. And non-pressure compensating emitters with vortex wash wall optimized flow path (NPCW) of the same flow rate were chosen. Similarly, pressure compensating emitters (PC) with two different discharges (1.0 L/h and 1.6 L/h) were selected. Both Table 1 and Fig. 2 display their flow path parameters and structures.

 # Fig. 1 approximately here #

 # Table 1 approximately here #

 # Fig. 2 approximately here #

2.2 Sampling and testing methods

2.2.1 Performance evaluation of drip irrigation emitter clogging

In this experiment, the discharges of 45 emitters were measured using the weighing method described by Feng et al. (2018). Given that outdoor tests are susceptible to environmental influences that may cause testing and measurement bias, the emitter discharges were corrected according to the water temperature at the time of testing, following Pei et al. (2014) procedure. Emitter clogging was assessed by computing the average discharge variation rate (Dra) according to Muhammad et al. (2021) and Ghaemi (1998).

$$Dra = \frac{\sum_{i}^{n} \frac{q_i^t}{q_i^0}}{n} \times 100\% \qquad (1)$$

In Eq.1 is the flow at the initial moment of No.i emitter, in L/h; is the flow at *t* hour of No.i emitter, in L/h; and n is the total number of emitter installed along the lateral.

2.2.2 Sampling and dry weight test of sediment

Following Liu et al. (2019), sampling and dry weight (DW) determination of the sediment granules were carried out using ultrasonic techniques to flake off the clogging substance present. DW was measured from 15 emitters, including 5 emitters at the beginning, in the middle and at the end of the drip irrigation unit, respectively. The detailed test methods are shown in the Supplementary Materials.

2.2.3 Concentration sample and test method

The sediment concentration was measured using the weighing method with 300 mL sampling bottles at the water source and emitter outlet, respectively, following the procedure described by Hou et al. (2022). Concentration was measured from 9 emitters, including 3 emitters were taken at the beginning, in the middle and at the end of the drip irrigation unit, respectively.

2.2.4 Particle size sample and test method

Following Hou et al. (2022), The sediment particle size was measured using the weighing method with 300 mL sampling bottles at the water source and emitter outlet. The detailed test methods are shown in the Supplementary Materials.

2.3 Evaluation index of the self-discharge capacity of sediment

2.3.1 Sediment discharge rate

The calculation formula for the sediment discharge rate φ_e for each type of emitter is shown in

Equation (1):

$$\varphi_e = \frac{\rho_i}{\rho_0} \times 100\% \quad (1)$$

Where, ρ_0 denotes the average value of irrigation water sediment concentration, g/L; and ρ_i represents the average value of sediment concentration of the *i* th emitter outflow, g/L.

2.3.2 Sediment deposition and discharge ratio

The calculation formula for the sediment deposition and discharge ratio φ is shown in Equation (2):

$$\varphi = \frac{\sum_{i=1}^{n} m_i \times n_i \times 15}{\sum_{i=1}^{n} \rho_i \times v_i} \times 100\% \quad (2)$$

Where, m_i is the average dry weight of clogging substances in emitter during the i-th flow measurement (each 15 m long), g/m; n_i is the corresponding number of emitter (each 15 m long drip irrigation unit); ρ_i is the *i* th emitter outflow sediment concentration, g/L; and v_i is the cumulative irrigation water volume, L.

2.3.3 Control threshold for the particle size

In order to explore the critical value of the sediment particle size discharged by different emitters, the distribution curve λ and the average line of total sediment discharge η were proposed for the interval of mass proportion of the sediment particle size discharged by emitters:

$$\eta = \frac{m}{M} \quad (3)$$

$$\lambda = \frac{m \times \mu_f}{M \times \mu} \quad (4)$$

Where, m refers to the average emitter discharge sediment dry weight, g; M is the total dry weight of sediment into the emitter, g; μ_f is the particle size distribution of the sediment discharged from the emitter, μm; and μ is the particle size distribution of sediment into the emitter, μm.

From the above Equations (3) and (4), the calculated data for NPCL1 emitter, as example, is shown in Fig. 3(a). When the emitter d the distribution curve λ is higher than the total sediment discharge average line η, the grain size interval mass ratio is considered positive (i.e., the emitter is releasing more solids than the average ratio of solids introduced), and the opposite, negative. Fig. 3(b) was obtained by integrating the difference between λ and η. The highest positive value in Fig. 3(b) corresponds to the particle size μ_0, which is defined as the maximum value when the sediment particle is easy to discharge from the emitter. That is, the critical threshold of the emitter sediment discharge particle size.

 # Fig. 3 approximately here #

2.4 Statistical analysis

Regression analysis was used to quantify the correlation among the Dra, sediment discharge capacity indicators, and structural parameters of the emitter. The significance of independent variables was determined at $p<0.05$. The forecasting model for the control threshold μ_0 was based in a multivariate linear relationship. The variance inflation factor (VIF) was used during the process of establishing the multivariate linear relationship between μ_0 and its influences to exclude the multi-collinearity among the influences. All the above statistical processes were performed using SPSS (version 17.0, IBM Analytics).

3. Results and analysis

3.1 Emitter clogging performance

The variation of the Dra for different types of emitters is shown in Fig. 4(a) under the working conditions of 0-75 μm and 3.0 g/L, while the rest of the working conditions are shown in the Supplementary Materials (Fig. S1). Fig. 4(b) shows the correlation of Dra of the different emitters regarding that of NPCL1. With the increase of the system's running time, Dra exhibited a trend of slow decline until around the 300 h of operation, followed by a rapid reduction. Besides, there were obvious differences between the different emitters. The PCE performed better than NPCE under the same flow conditions. Overall, under the same flow conditions, the Dra of PCE was improved by 16.9%-33.0% compared with the different NPCL emitters, and 23.0%-32.8% regarding the NPCW emitters. Among NPCE, the NPCW performed better, showing Dra 10.7%-14.1% higher than those of NPCL. Emitters at different flow rates presented different trends. At a flow rate of 1.0 L/h, the Dra of the NPCW and the PC emitters was improved by 13.1% and 33.0%, respectively, when compared with the NPCL1 emitter. However, at a flow rate of 1.6 L/h, NPCW3 and PC3 emitters only improved Dra by 14.1% and 16.9%, respectively, regarding NPCL3.

 # Fig. 4 approximately here #

3.2 Control threshold for particle size μ_0

The relative variation of the control threshold for particle size μ_0 for different types of emitters is shown in Fig. 5(a) under the working conditions of 0-75 μm and 3.0 g/L. The evolution of the control threshold for the rest of experimental conditions is shown in the Supplementary Materials (Fig. S2), while Fig. 5(b) shows the correlation between μ_0 for NPCL1 and the other emitters tested. With the increase of the system's running time, μ_0 exhibited a declining trend, appearing obvious differences between emitters. Under the same flow conditions, PCE had higher μ_0 than NPCE. Overall, μ_0 of PCE was improved by 1.4%-21.3% compared with the NPCL emitters, and it was 0.2%-7.61% when compared with the NPCW emitters. Among NPCE, the μ_0 of the NPCW emitters was larger than that of the NPCL, with an average improvement rate of 0.9%-14.2%. At the same time, emitters at different flow rates present different trends. At a flow rate of 1.0 L/h, the NPCW1 and the PC1 emitters improved μ_0 regarding NPCL1 by 2.1%-14.2% and 4.1%-21.3%, respectively, while at a flow rate of 1.6 L/h, the NPCW3 and PC3 emitters increased μ_0 by 0.9%-3.2% and 1.4%-2.8%, respectively. With the accumulated system operation, the control threshold value of the sediment discharge particle size of different types of emitters gradually decreased. With the increase of sediment concentration and particle size of the water source, the control threshold value of the sediment discharge particle size presents a decreasing and increasing trend, respectively (Supplementary Materials, Fig. S3). Further, control threshold for particle size was more influenced by particle size than concentration.

 # Fig. 5 approximately here #

3.3 Sediment discharge rate (φ_e)

The relative variation of the φ_e for the different types of emitters under the working conditions of 0-75 μm and 3.0 g/L is shown in Fig. 6(a). Results for the other working conditions are shown in the Supplementary Materials (Fig. S4). Fig. 6(b) depicts the correlations of φ_e between each emitter and NPCL1. With the increase of the system's running time, φ_e exhibited an increasing trend first and then a decrease. The sediments discharge rate of each emitter reached the maximum value when the system operated 200-400 h. Besides, there are obvious differences between different emitters. Under the same flow conditions, φ_e of PCE was higher than that of NPCE. Overall, φ_e of PCE was improved by -0.4%-2.7% compared with the NPCL emitters and -0.9%-1.2% compared with the NPCW emitters. For NPCE, the NPCW emitter performed better than the NPCL emitter, with a relative improvement of φ_e in the range -0.8%-2.3%. Besides, emitters at different flow rates presented different trends. At a flow rate of 1.0 L/h, the φ_e of the NPCW1 and the PC1 emitters were improved by -0.2%-2.3% and -0.1%-2.7%, respectively. Compared with the NPCL1, while at a flow rate of 1.6L/h, φ_e of the NPCW3 and the PC3 emitter were improved by -0.8%-0.7% and -0.9%-

0.6%, respectively. With the increase of the sediment concentration and particle size of the water source, the control threshold value of the sediment discharge particle size presents a trend of increasing and then decreasing, respectively (Supplementary Materials, Fig. S4).

 # Fig. 6 approximately here #

3.4 Sediment deposition and discharge ratio (φ)

The relative variation of φ for the different types of emitters is shown in Fig. 7(a) under the working conditions of 0-75 μm and 3.0 g/L. In the Supplementary Materials, Fig. S5 represents the rest of experimental conditions. It is shown that the emitter discharges more than 99% of sediment particles that enter it. Fig.7(b) depicts the correlation for φ between each emitter and NPCL1. With the increase of the system's running time, φ exhibited an increasing trend first and then decreasing, but there were clear differences between different emitters. Under the same conditions, the φ of PCE is lower than NPCE. Overall, the relative effect of PCE was improved by 0.1%-69.8%, among which, the effect was improved by 11.5%-69.8% compared with the NPCL emitters and 0.1%-42.2% compared with the NPCW emitters. For NPCE, the NPCW emitter performed better than the NPCL emitter, with a φ relative improved by 9.4%-50.7%. Besides, emitters at different flow rates presented different trends. At a flow rate of 1.0 L/h, the φ of the NPCW1 and the PC1 emitters were improved by 14.7%-43.7% and 35.1%-67.6%, respectively, compared with the NPCL1, while at a flow rate of 1.6 L/h, those of the NPCW3 and the PC3 emitters were improved by 9.4%-29.6% and 11.5%-34.4%, respectively. With the increase of the sediment concentration of the water source, the control threshold value for particle size presented a decreasing trend. (Fig. S5).

 # Fig. 7 approximately here #

3.5 Influence of NPC emitter geometry parameters and indicators for the sediment self-discharge capacity

For NPCE, the influence of structural parameters and water source parameters on the indicators of the self-discharge capacity of the emitter is shown in Fig. 8. Among the structural parameters, there was a significant correlation between the emitter channel length (L), the ratio of the cross-sectional area to the length ($\sqrt{A}/L$), the section mean flow velocity (v), the rated flow rate (Q) and three self-discharge sediment indicators. Among the water source parameters, the particle size, and the concentration had significant effects on the indicators of self-discharge capacity of the emitter. Taking the control threshold for particle size μ_0 as an example, a forecasting model for the control threshold μ_0 was constructed with its structural parameters (length of flow path (L), ratio of cross-sectional area of flow path open to length ($\sqrt{A}/L$), section mean flow velocity (v), and rated flow rate (Q) as variables. As it is greatly influenced by the particle size gradation of the water source, μ_0 varies within 6% under different concentration conditions (Fig. S6). Consequently, under the operating conditions of this experiment, prediction models for emitter sediment discharge particles by each of the three different sediment gradations (0-41 μm, 0-75 μm, and 0-100 μm) were obtained as shown in Equations (5-7) (p<0.05).

 # Fig. 8 approximately here #

$$\mu_0 = 128.16 \times \sqrt{A}/L - 0.29 \times L + 0.29 \times v + 1.37 \times Q + 30.53 \quad \text{(0-41 μm, P<0.05)} \tag{5}$$

$$\mu_0 = 120.00 \times \sqrt{A}/L - 0.21 \times L + 0.75 \times v + 1.27 \times Q + 56.28 \quad \text{(0- 75 μm, P<0.05)} \tag{6}$$

$$\mu_0 = 121.79 \times \sqrt{A}/L - 0.21 \times L + 0.62 \times v + 1.29 \times Q + 62.30 \quad \text{(0-100 μm, P<0.05)} \tag{7}$$

Where, $\sqrt{A}/L$, the flow path cross-sectional area opening to length; L, the channel length, mm; v, the flow velocity, m/s; and Q, the emitter flow rate, L/h.

4. Discussion

4.1 Emitter self-discharge sediment mechanism

It is hereby discovered that the total amount of sediment deposited inside the emitter was 0.3-1.1g when it was operated up to 640h, and the total amount of sediment entering the emitter during the operation time (the product of the outflow flow rate of the emitter and the concentration of solid suspended particles in the water source) was about 384.2-1843.2g, which means that more than 99% of sediment particles (< 100 μm) was discharged out through the emitter, indicating the effectiveness of the emitter in removing sediment. The sediment discharge rate φ_e was between 36%-52%, this indicates that 36%-52% of the water source sediment is discharged from the drip irrigation system through the emitter, while the remaining 48%-64% sediment is discharged through the drip irrigation belt flushing or siltation in the belt. But the sediment deposition and discharge ratio φ (i.e., the percentage of the sediment entering the emitter which is silted up in the emitter) was between 0.01%-0.12%, and the rest of the sediment was discharged through flushing or silted up in the drip irrigation pipe. This finding also demonstrates the possibility of modifying the current conception of drip irrigation systems so that small particles of sediment can be discharged directly through the emitter rather than intercepting them through a filtration system, thereby reducing the requirement for a filtration system. Both the sediment deposition discharge ratio and emitter sediment discharge rate exhibit a rising and then falling trend with the system operation time going by. Besides, both the sediment deposition and discharge ratio φ and sediment discharge rate φ_e rise at first and fall then with system operation time. Additionally, the initial operation of the system φ and φ_e shows a rising trend due to the emitter and drip irrigation pipe sediment particles and wall collision adhesion, while the sediment surface microbial adhesion growth maybe enhances the sediment particles by the adsorption force (Shen et al, 2022; Song et al, 2017; Guan et al, 2018). In the middle and late system operating stage, the emitter internal fouling increased gradually, reducing the cross-sectional area of the flow path, so that the adhering sediment particles with enhanced water flow shear force effect were gradually flushed out of the emitter (Zhou et al, 2021; Li et al, 2015), and the sediment deposition and discharge ratio φ and sediment discharge rate $φ_e$ declined slowly. With the system operating time going by, the control threshold for particle size $μ_0$ showed a gradually decreasing trend, maybe because additional particle retention effect caused by previously settled particles, and large sediment particles are more likely to be wall captured and adsorbed. (Xiao et al, 2020).

The emitter sediment discharge rate decreases with higher water source particle sizes. Conversely, the sediment deposition discharge ratio, and the control threshold of sediment discharge particle size present an increasing trend. The reason is mainly because, at the same flow rate, larger particles could be easily settled in the pipe and water is not conveyed better within the emitter channel (Hou et al, 2022), and, consequently, the degree of emitter clogging is worsened. As more sediment is deposited, the rate at which sediment is discharged from the emitter is lowered, and therefore sediment deposition discharge ratio is increased. At the same time, given that more than 99% of the sediment smaller than 100 μm entering the emitter can be discharged from it, the sediment discharge particle size control threshold rises with an increase in the water source particle size. However, as the water source concentration decreases, the sediment discharge rate, and the control threshold of sediment discharge particle size of the emitter decrease while the sediment deposition discharge ratio increases. This is because the sediment concentration in the water source increases, and the chance of collision between the particles and between the wall and its particles increases as well, which increases the chance of adhesion between the sediment particles and the emitter wall and each other (Yao et al, 2016;Wu et al, 2014), thereby exacerbating the risk of emitter clogging, and eventually leading to the decrease of the emitter sediment discharge rate and the control threshold of the sediment discharge particle size, and the increase of the sediment deposition discharge ratio.

4.2 Selection of the emitter self-drainage sediment capacity indicators

It is hereby discovered that the variation in water source particle size has a much greater impact on discharged particle size than the variation in concentration, which is mainly because the water source particle size determines the internal particle size distribution into the emitter. At the same time, the critical threshold of discharge particle size is more influenced by the emitter flow path internal water flow rate. The fine sediment particles are conveyed better with the water flow and can be directly discharged with the water, and they are therefore less affected by the concentration. The water source particle size and water source concentration have the same degree of impact on the sediment discharge rate φ_e, mainly because large particles of sediment are more difficult to discharge with the water due to the increase in water source particle size. Besides, the change in the water source concentration exercises a much greater influence on the sediment deposition discharge ratio φ_e than that in particle size, which is primarily attributed to the poor flowing performance of coarse sediment particles with the water, and most of the particles will be deposited in the capillary internal, without flowing into the emitter. When fine sediment particles of higher concentration flow into the emitter, the probability of its collision and adhesion with the wall of the emitter channel is doubled (Zhou et al, 2021), thereby leading to the sediment accumulation.

Fitting analysis was conducted on the sediment self-discharge capacity of the three indicators under identical working conditions (Fig. 9). Significant linear correlations (p<0.05) were found among the sediment deposition and discharge ratio, the sediment discharge rate, and the control threshold for particle size, indicating that the trend of each indicator was consistent. In this case, any indicator can represent the relatively high or low sediment discharge capacity of the emitter. Given that the control threshold of the discharge particle size can be used to direct the control particle size of the first filtration device, it is considered the primary indicator for determining the sediment discharge capacity of the emitter.

 # Fig. 9 approximately here #

4.3 Emitter selection

It is hereby found that, among different emitters, PCE perform better than NPCE, while among the NPCE, the NPCW emitters perform better than the NPCL emitters. The elastic diaphragm in the pressure-compensating emitter can alter the outflow path's cross-sectional area, thus making impurity particles easier to flush out under variable flow path conditions (El Bouhali et al., 2020; Wei et al., 2014), Therefore, the pressure-compensating emitters are provided with a relatively high sediment discharge capacity. However, in non-pressure compensating emitters, the flow path structure parameters are different. Besides, it is also observed that the flow path length of the emitter (L), the ratio of the flow path cross-sectional area opening to length ($\sqrt{A}/L$), section average flow velocity (v), and rated flow rate (Q) have a significant effect on the self-discharge sediment capacity of the emitter. The main reason is that the longer the flow path (L) is, the sediment-discharging ability of the emitter becomes weaker, and the collision time of solid particles becomes longer. Besides, the friction with the flow path wall is larger, and it gets easier to silt in the flow path. Additionally, $\sqrt{A}/L$ reflects the characteristics of the cross-sectional area and length of the flow path, with a larger value indicating a stronger relative sediment-carrying capacity of the internal water flow. A greater Q implies a higher flow rate in the pipe lumen, a higher sediment-carrying capacity, and a better sediment discharge effect, being the shear force in the flow path higher with the increase of the average flow velocity (v) of the section. As a result, more sediment is discharged from the emitter and less clogging material is deposited in the flow path when the sediment particles are stripped and flushed out (Feng et al., 2018; Ustun et al., 2012; Wang et al., 2009).

It can be seen from Fig. 8 that there is no relationship between the self-discharge sediment capacity and flow index (x) of the emitter in this study, but some studies have proposed that the anti-clogging performance of the emitter has a relationship with the flow index (x) because the flow index can reflect the degree of fluid turbulence in the labyrinth channel of the emitter to a certain extent (Wei et al., 2008; Zhou et al., 2019), this is mainly due to the fact that the flow indices of the different emitters are in the range of 0.50-0.53, and did not test for changes in flow indices with running time. Therefore, there is no relationship between the self-discharge sediment capacity and flow index (x).

The forecast model for the control threshold of the emitter sediment discharge particle size is hereby developed as shown in Equations 5-7, which can serve as a theoretical foundation for the design of high sediment self-discharge capacity emitters and guide the initial filter equipment arrangement. However, this paper only analyzes the self-discharge capacity of a sole source using the Yellow River water, but fertilization and other factors will also have an impact on the sediment movement within driplines and emitters. To this end, differences in the self-discharge capacity of the emitters still need to be further explored under fertilized conditions.

5. Conclusions

Based on the findings of this study, the main conclusions are drawn as follows:

(1) The majority (>99%) of the fine particles (<100 μm) of sediment entering the drip irrigation emitter can be discharged through the flow path, indicating the effectiveness of the emitter in removing sediment. Among them, 36%-52% of the water source sediment is discharged from the drip irrigation system through the emitter, while the remaining 48%-64% sediment is discharged through the drip irrigation belt flushing or siltation in the belt.

(2) Under the same flow conditions, PCE had higher μ0 than NPCE. Overall, μ0 of PCE was improved by 1.4%-21.3% compared with the NPCL emitters, and it was 0.2%-7.61% when compared with the NPCW emitters. Among NPCE, the μ0 of the NPCW emitters was larger than that of the NPCL, with an average improvement rate of 0.9%-14.2%.

(3) The self-discharge sediment capacity of NPCE was mainly affected by the emitter flow path length (L) and the ratio of the flow path cross-sectional area open square to length ($\sqrt{A}/L$). The SDC of the emitter can be improved by enhancing the average flow velocity of the section (v) and rated flow rate (Q).

Acknowledgements

We appreciate the financial support from the National Natural Science Foundation of China (51790531, 51621061).

Compliance with ethical standards

Conflict of interest: On behalf of all authors, the corresponding author states that there is no conflict of interest.

References

Bové J, Puig-Bargués J, Arbat G et al (2017) Development of a new underdrain for improving the efficiency of micro irrigation sand media filters. Agric. Water Manage. 179, 296-305. https://doi.org/10.1016/j.agwat. 2016.06.031.

Capra A, Scicolone B (2004) Emitter and filter tests for wastewater reuse by drip irrigation. Agric. Water Manage. 68(2), 135-149. https://doi.org/10.1016/j.agwat.2004.03.005.

Duker A, Cambaza C, Saveca P et al (2020) Using nature-based water storage for smallholder irrigated agriculture in African drylands: Lessons from frugal innovation pilots in Mozambique and Zimbabwe. Environ Sci Policy. 107, 1-6. https://doi.org/10.1016/j.envsci.2020.02.010.

El-Bouhali M, Ouarriche H, Bouisfi F et al (2020) Clogging investigation of pressure compensating button emitters: an experimental study of four types. Environ Sci Pollut R. 27(35), 44325-44332. https://doi.org/10.1007/s11356-020-10299-w.

Feng J, Li YK, Wang WN et al (2018) Effect of optimization forms of flow path on emitter hydraulic and anti-clogging performance in drip irrigation system. Irrigation Sci. 36(1), 37-47. https://doi.org/10.1007/s00271-017-0561-9.

Ghaemi A (1998) Impact of different patterns of emitter clogging on hydraulic characteristics of micro irrigation laterals laid on flat and sloped terrains. The university of British Columbia. https://doi.org/10.14288/1.0058701

Guan YH, Niu WQ, Liu L et al (2018) Effect of fertilizer type and concentration on sediment transport capacity of dripper in drip fertigation with muddy water. Trans Chin Soc Agric Eng. 34(1), 78-84. https://doi.org/10.11975/j.issn.1002-6819.2018.01.011.

Han S Q, Li YK, Zhou B et al (2019) An in-situ accelerated experimental testing method for drip irrigation emitter clogging with inferior water. Agric. Water Manage. 212, 136-154. https://doi.org/10.1016/j.agwat.2018.08.024.

Hou P, Puig-Bargués J, Xiao Y et al (2022) An improved design of irrigation centrifugal filter for separating water and fine sediment: appropriately increase head loss for high efficiency. Irrigation Sci. 40(2), 151-161. https://doi.org/10.1007/s00271-021-00765-9.

International Organization for Standardization (2004) Geneva. ISO 9261: Agricultural irrigation equipment –emitters and emitting pipe: Specificationsand test methods.

Li YK, Song P, Pei YT et al (2015) Effects of lateral flushing on emitter clogging and biofilm components in drip irrigation systems with reclaimed water. Irrigation Sci. 33(3), 235-245. https://doi.org/10.1007/s00271-015-0462-8.

Liu L, Niu WQ, Bob Z et al (2012) Influence of sediment particle size on clogging performance of labyrinth path emitters. Trans Chin Soc Agric Eng. 28(1), 87-93. https://doi.org/10.3969/j.issn.1002-6819.2012.01.017.

Liu ZY, Xiao Y, Li YK et al (2019) Influence of operating pressure on emitter anti-clogging performance of drip irrigation system with high-sediment water. Agric. Water Manage. 213: 174-184. https://doi.org/10.1016/j.agwat.2018.10.017

Muhammad T, Zhou B, Liu ZY et al (2021) Effects of phosphorus-fertigation on emitter clogging in drip irrigation system with saline water. Agric. Water Manage. 243, 106392. https://doi.org/10.1016/j.agwat.2020.106392.

Niu WQ, Liu L, Chen X et al (2013) Influence of fine particle size and concentration on the clogging of labyrinth emitters. Irrigation Sci. 31(4), 545-555. https://doi.org/10.1007/s00271-012-0328-2.

Pei YT, Li YK, Liu YZ et al (2014) Eight emitters clogging characteristics and its suitability under on-site reclaimed water drip irrigation. Irrigation Sci. 32(2), 141-157.

https://doi.org/10.1007/s00271-013-0420-2.

Puertes C, Bautista I, Lidón A et al (2021) Best management practices scenario analysis to reduce agricultural nitrogen loads and sediment yield to the semiarid Mar Menor coastal lagoon (Spain). Agr Syst. 188, 103029. https://doi.org/10.1016/j.agsy.2020.103029.

Puig-Bargués J, Lamm FR (2013) Effect of flushing velocity and flushing duration on sediment transport in micro irrigation driplines. Trans ASABE. 56, 1821-1828. https://doi.org/10.13031/trans.56.10293.

Qin Y, Mueller ND, Siebert S et al (2019) Flexibility and intensity of global water use. Nat Sustain. 2(6), 515-523. https://doi.org/10.1038/s41893-019-0337-8.

Shen Y, Puig-Bargues J, Li MY et al (2022) Physical, chemical and biological emitter clogging behaviors in drip irrigation systems using high-sediment loaded water. Agric. Water Manage. 270, 107738. https://doi.org/10.1016/j.agwat.2022.107738.

Song P, Li YK, Zhou B et al (2017) Controlling mechanism of chlorination on emitter bio-clogging for drip irrigation using reclaimed water. Agric. Water Manage. 184, 36-45. https://doi.org/10.1016/j.agwat.2016.12.01.

Tao HF, Yang HH, Ma YJ et al (2017) Influence of flow rate on flow velocity distribution in gravity sinking and filter tank for drip irrigation with river water. Trans Chin Soc Agric Eng. 33(1), 131-137. https://doi.org/10.11975/j.issn.1002-6819.2017.01.018.

Ustun S, Talip T, Seçkin E et al (2012) Evaluation of $CaCO_3$ Clogging in Emitters with Magnetized Saline Waters. Desalin Water Treat. 40(1), 168-173. https://doi.org/10.5004/dwt.2012.2845.

Wang WE, Wang FJ, Niu WQ et al (2009) Numerical analysis of influence of emitter channel structure on suspended granule distribution. Trans Chin Soc Agric Eng. 25(5), 1-6.

https://doi.org/10.3969/J.ISSN.1002-6819.2009.5.001.
Wei QS, Lu G, Liu J et al (2008) Evaluations of emitter clogging in drip irrigation by two-phase flow simulations and laboratory experiments. Comput. Electron. Agric. 63 (2), 294–303. https://doi.org/10.1016/j.compag.2008.03.008.
Wei ZY, Yuan WJ, Zhou X et al (2014) Research progress of pressure compensating emitters in micro-irrigation systems in China. Trans Chin Soc Agric Mach. 45(1), 94-101+107. https://doi.org/10.6041/j.issn.1000-1298.2014.01.016.
Wu ZG, Zhang ZT, Zhang KM et al (2014) Influence of particle size and concentration of sediment on clogging of labyrinth channels emitters. Trans Chin Soc Agric Eng. 30(7), 99-108. https://doi.org/10.3969/j.issn.1002-6819.2014.07.012.
Xiao Y, Sawicka B, Liu Y et al (2020) Visualizing the macroscale spatial distributions of biofilms in complex flow channels using industrial computed tomography. Biofouling. 36(2), 115-125. https://doi.org/10.1080/08927014.2020.1728260.
Yao HF, Shi, CX, Shao WW et al (2016) Changes and influencing factors of the sediment load in the Xiliugou basin of the upper Yellow River, China. Catena. 142, 1-10. https://doi.org/10.1016/j.catena.2016.02.007.
Zeng XT, Chen C, Liu AH et al (2018) Planning a sustainable regional irrigated production and forest protection under land and water stresses with multiple uncertainties. J Clean Prod. 188, 751-762. https://doi.org/10.1016/j.jclepro.2018.04.028.
Zhang RC, Niu WQ, Duan XH et al (2017) Optimization of drip irrigation uniformity model considering location of clogged emitters. Trans Chin Soc Agric Eng. 33(3), 113-120. https://doi.org/10.11975/j.issn.1002-6819.2017.03.015.

Zhang WQ, Lv C, Zhao X et al (2021) The influence mechanism of the main suspended particles of Yellow River sand on the emitter clogging − An attempt to improve the irrigation water utilization efficiency in Yellow River basin. Agric. Water Manage. 258, 107202. https://doi.org/10.1016/j.agwat.2021.107202.

Zhou B, Li YK, Xue S et al (2019) Variation of microorganisms in drip irrigation systems using high-sand surface water. Agric. Water Manage. 218, 37-47. https://doi.org/10.1016/j.agwat.2019.02.038

Zhou B, Hou P, Xiao Y et al (2021) Visualizing, quantifying, and controlling local hydrodynamic effects on biofilm accumulation in complex flow paths. J Hazard Mater. 416, 125937. https://doi.org/10.1016/j.jhazmat.2021.125937.

Zhou HX, Li YK, Wang Y et al (2021) Composite fouling of drip emitters applying surface water with high sand concentration: Dynamic variation and formation mechanism. Agric. Water Manage. 215, 25-43. https://doi.org/10.1016/j.agwat.2019.01.009.

Captions for figures involved in this paper

Fig. 1 Layout of the experimental system.

Fig. 2 Structure of different drip irrigation emitters tested.

Fig. 3 Control threshold for the particle size of the high-sediment water.

Fig. 4 Average discharge variation rate (Dra).

Fig. 5 Control threshold for particle size (μ_0).

Fig. 6 Sediment discharge rate (φ_e).

Fig. 7 Sediment deposition and discharge ratio (φ).

Fig. 8 Correlation between indicators of emitter self-discharge sediment capacity and structural parameters.

Fig. 9 Emitter self-discharge sediment indicator selection.

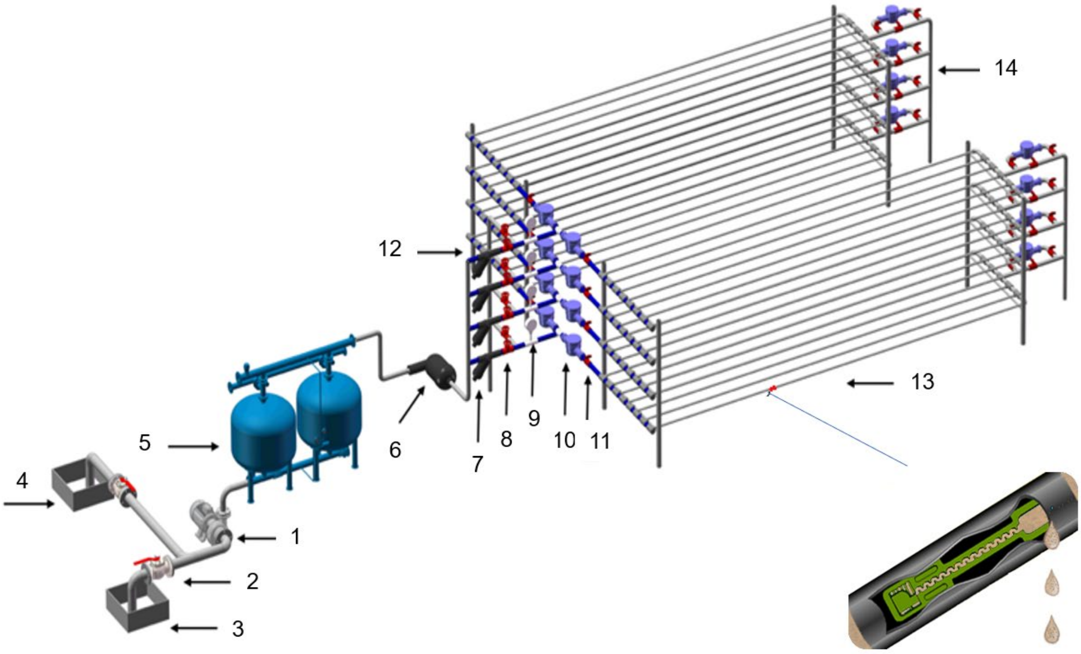

Fig. 1. Layout of the experimental system. The experimental setup is consistent with Muhammad et al. (2021), 1. Water pump; 2. Butterfly valve; 3, 4. Reservoir; 5. Sand filter; 6. Disc filter (100 mesh); 7. Small disc filter (100 mesh); 8, 11. Fine adjustment valve; 9. Pressure gauge; 10. Water meter; 12. Return pipe; 13. Drip irrigation pipe; 14. Flushing device

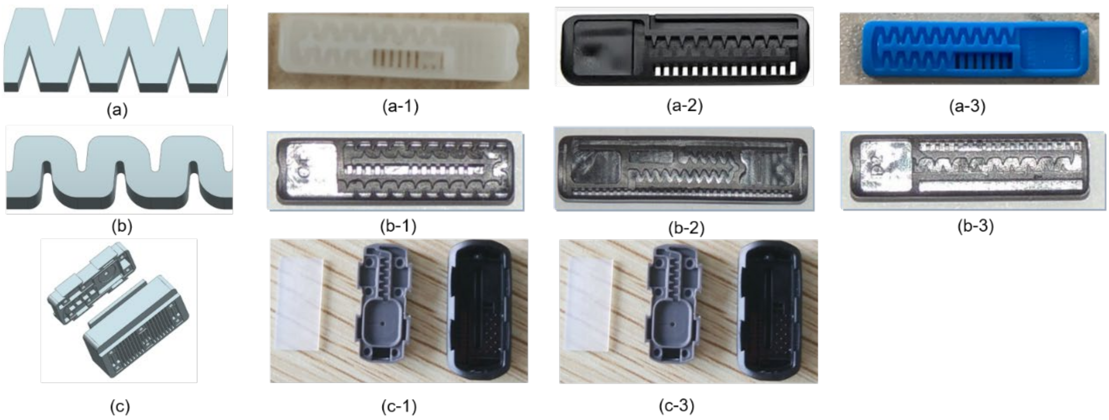

Fig. 2. Structure of the different emitters tested. (a) NPCL structure, (a-1) NPCL1, (a-2) NPCL2, (a-3) NPCL3, (b) NPCW structure, (b-1) NPCW1, (b-2) NPCW2, (b-3) NPCW3, (c) PC structure, (c-1) PC1, (c-2) PC2.

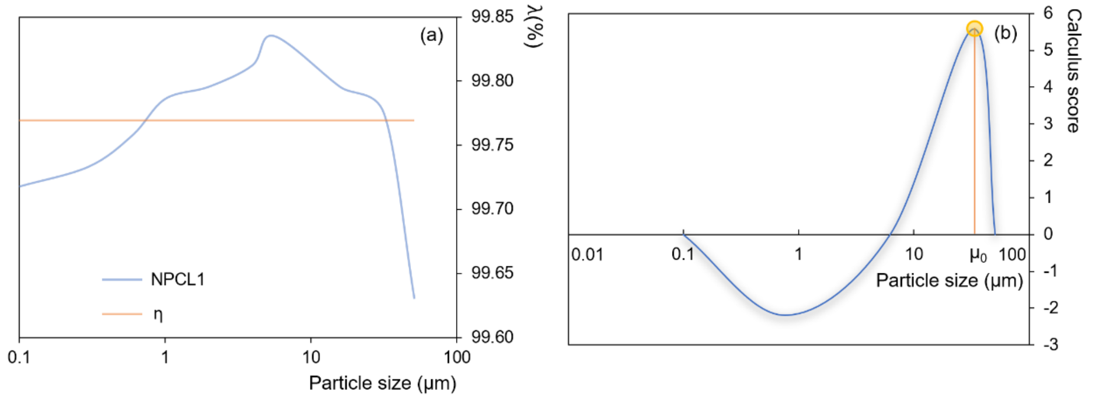

Fig. 3. Control threshold for particle size, (a) the distribution curve λ, η is total sand discharge, (b) Integrating the difference between λ and η, μ_0 is control threshold for particle size.

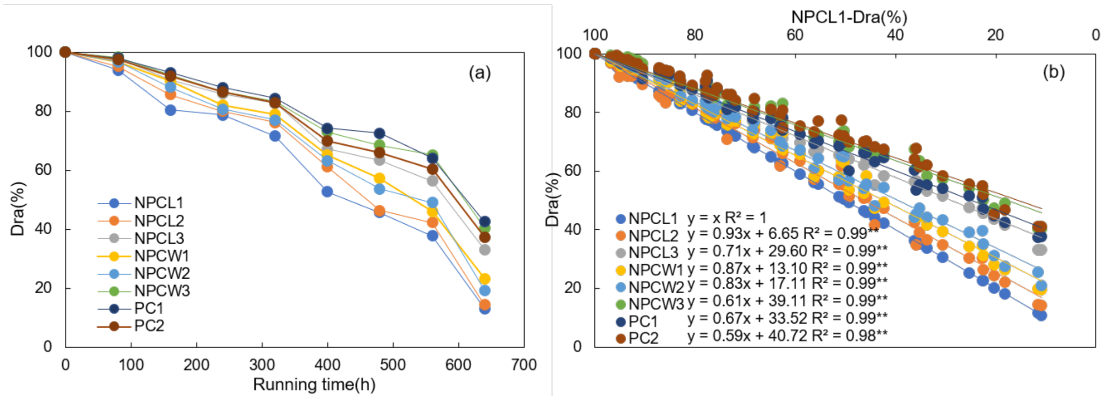

Fig. 4. Average discharge variation rate (Dra). Evolution of average discharge variation rate (Dra) under the sediment diameter of 0-75 μm and sediment concentration of 3.0 g/L is shown in (a), while the rest of the working conditions are shown in the Supplementary Material Fig. S1. Regression analysis of Dra for each type of emitters regarding of NPCL1 is shown in (b), and ** represents significant level $p < 0.01$.

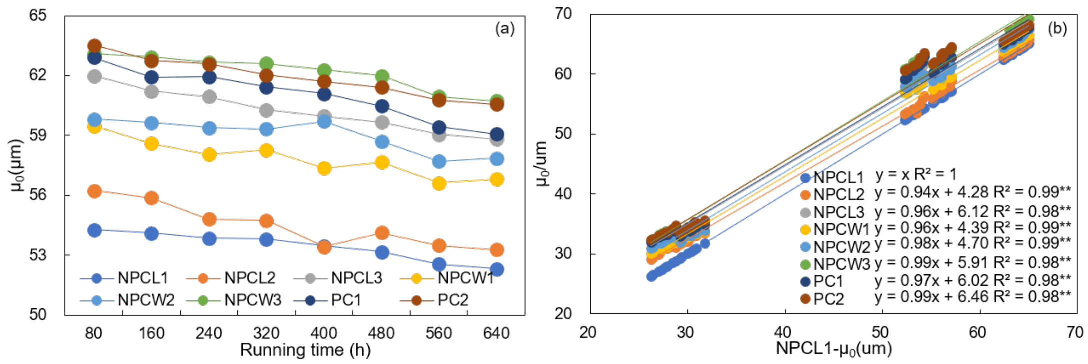

Fig. 5. Control threshold for particle size (μ_0). Evolution of the control threshold for particle size (μ_0) under the sediment diameter of 0-75 μm and sediment concentration of 3.0 g/L is shown in (a), while the rest of the working conditions are shown in the Supplementary Material Fig. S3. Regression analysis of μ_0 for each type of emitters regarding of NPCL1 is shown in (b), and ** represents significant level $p < 0.01$.

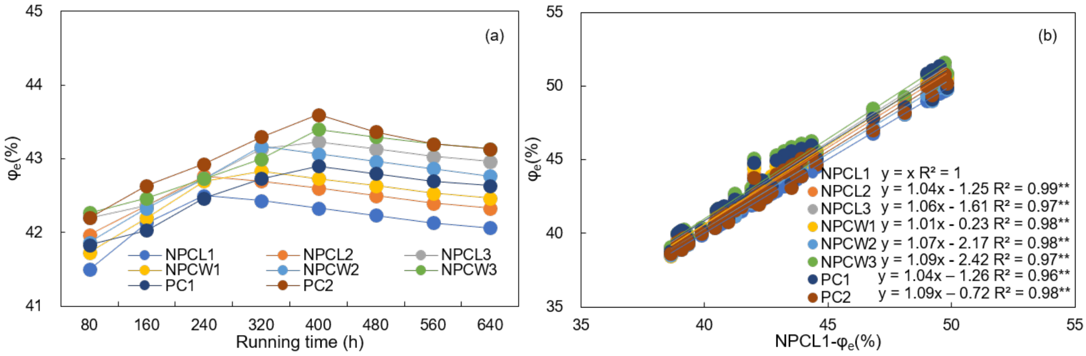

Fig. 6. Sediment discharge rate (φ_e). **Evolution of the sediment discharge rate (φ_e) under the sediment diameter of 0-75 μm and sediment concentration of 3.0 g/L is shown in (a), while the rest of the working conditions are shown in the Supplementary Material Fig. S4. Regression analysis of μ_0 for each type of emitters regarding of NPCL1 is shown in (b), and ** represents significant level $p < 0.01$.**

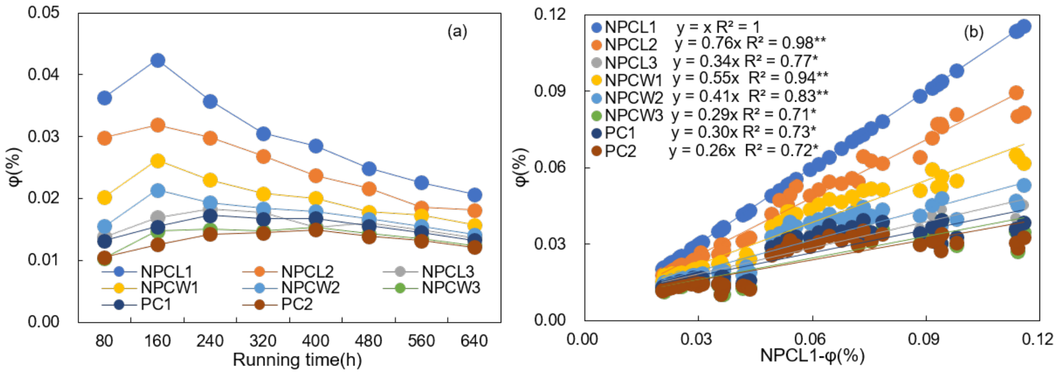

Fig. 7. Sediment deposition and discharge ratio (φ). Evolution of the sediment deposition and discharge ratio (φ) under the sediment diameter of 0-75 μm and sediment concentration of 3.0 g/L is shown in (a), while the rest of the working conditions are shown in the Supplementary Material Fig. S5. Regression analysis of μ_0 for each type of emitters regarding of NPCL1 is shown in (b), and ** represents significant level $p < 0.01$.

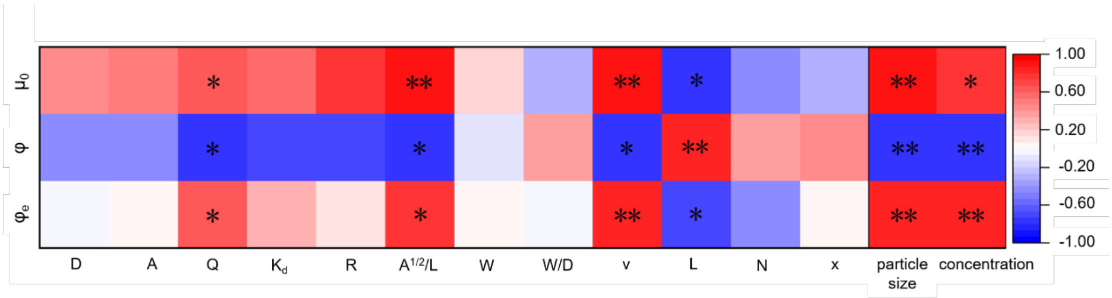

Fig. 8 Correlation between indicators of emitter self-discharge sediment capacity and structural parameters. L, W, D represents flow path length, width and channel depth, respectively, mm; A represents cross-sectional area of channel, mm^2; Q represents emitter flow rate, L/h; K_d represents flow rate coefficient; R represents channel wetted perimeter, （mm）; *v* represents flow velocity, （m/s）; N represents number of channel units; *x* represents flow index. ** represents $p < 0.01$, and * represents $p < 0.05$.

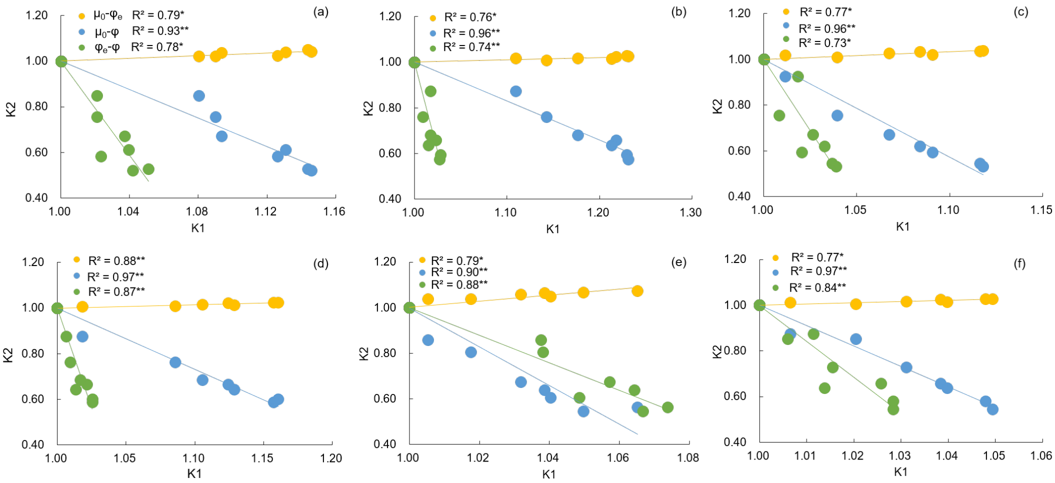

Fig. 9. Emitter self-discharge sediment indicator selection. K1 and K2 are the index (μ_0, φ, φ_e) ratio of different emitters to NPCL1 emitter. (a-f) are the results under the working conditions of 0-41 μm and 1.0 g/L, 0-41 μm and 3.0 g/L, 0-75 μm and 1.0 g/L, 0-75 μm and 3.0 g/L, 0-100 μm and 1.0 g/L, 0-100μm and 3.0 g/L, respectively.

Table 1 Characteristics of drip irrigation emitters applied

No.	Flow rate (L/h)	flow rate coefficient	flow index	channel wetted perimeter	flow velocity	number of channel units	Geometrical parameters of the flow path			Wall thickness (mm)	Manufacturer location	Abbreviation
							Length (mm)	Width (mm)	Depth (mm)			
1	1.0	3.39	0.53	3.33	0.25	9	47.13	0.91	1.21	0.20	China	NPCL1
2	1.4	4.64	0.52	2.17	0.68	9	35.52	0.89	0.64	0.20	China	NPCL2
3	1.6	5.06	0.5	1.98	0.93	14	22.83	0.82	0.58	0.20	Israel	NPCL3
4	1.0	3.16	0.5	2.16	0.54	18	40.36	0.72	0.72	0.15	China	NPCW1
5	1.4	4.74	0.53	2.17	0.76	14	37.79	0.69	0.74	0.15	China	NPCW2
6	1.6	5.3	0.52	1.96	1.54	9	23.50	0.36	0.80	0.15	China	NPCW3
7	1.0	1.05	0.02	3.05	0.32	5	14.42	0.77	1.14	0.38	Israel	PC1
8	1.6	1.68	0.02	2.65	0.63	5	18.17	0.73	0.96	0.38	Israel	PC2

Note: PC is pressure compensating emitter, NPCL is non-pressure compensating emitters (NPC) with toothed flow path, NPCW is non-pressure compensating emitters with vortex wash wall optimized.